Spectroscopic, Thermal and Biological Studies of the Coordination Compounds of Sulfasalazine Drug: Mn(II), Hg(II), Cr(III), ZrO(II), VO(II) and Y(III) Transition Metal Complexes

Mohamed Gamal ABD EL-WAHED,[a] Moamen Salah REFAT,*,[b] and Samy Mohamed EL-MEGHARBEL[a]

[a] *Department of Chemistry, Faculty of Science, Zagazig University; Zagazig 44111, Egypt: and* [b] *Department of Chemistry, Faculty of Science, Port Said, Suez Canal University; Port Said 42111, Egypt.*

Received July 20, 2008; accepted August 21, 2008; published online August 25, 2008

The complexations of sulfasalazine (H_3Suz) with some of transition metals have been investigated. Three types of complexes, $[Mn(HSuz)^{-2}(H_2O)_4]\cdot 2H_2O$, $[M(HSuz)^{-2}(H_2O)_2]\cdot xH_2O$ (M=Hg(II), ZrO(II) and VO(II), x=4, 8 and 6, respectively) and $[M(HSuz)^{-2}(Cl)(H_2O)_3]\cdot xH_2O$ (M=Cr(III) and Y(III), x=5 and 6, respectively) were obtained and characterized by physicochemical and spectroscopic methods. The IR spectra of the complexes suggest that the H_3Suz behaves as a bidentate ligand. The thermal decomposition of the complexes as well as thermodynamic parameters (ΔE^*, ΔH^*, ΔS^* and ΔG^*) were estimated using Coats–Redfern and Horowitz–Metzger equations. *In vitro* antimicrobial activities of the H_3Suz and the complexes were tested.

Key words infrared spectrum; electronic spectrum; thermal analysis; sulfasalazine; antimicrobial activity

Sulfasalazine (Fig. 1, H_3Suz) is a sulfa drug, a derivative of mesalazine (5-aminosalicylic acid abbreviated as 5-ASA), used primarily as an anti-inflammatory agent in the treatment of inflammatory bowel disease as well as for rheumatoid arthritis.[1—4)]

When dealing with the interaction between drugs and metal ions in living systems, a particular interest has been given to the interaction of metal ions with antibiotics. Antibiotics that interact with metal ions constitute a class of drugs which has been widely used in medicine both towards human beings and animals.[5,6)] In particular, the interaction between transition metals and β-lactamic antibiotics such as cephalexin has been recently investigated by several physicochemical and spectroscopic methods, and with detailed biological data.[7—10)] Many drugs possess modified pharmacological and toxicological properties when administered in the form of metallic complexes. Probably the most widely studied cation in this respect is Cu(II), since a host of low-molecular-weight copper complexes have been proven beneficial against several diseases such as tuberculosis, rheumatoid, gastric ulcers, and cancers.[11—14)]

In the literature survey, there is little attention concerning the mode of coordination of H_3Suz with metal ions. Previous studies[15—22)] of the complexation of sulfa drugs did not focus on the coordination behavior, but only dealt with the solution state and crystal structures of its metal complexes.

In our previous work respecting metal drug complexes, the synthesis, structural, thermal and biological studies of folic acid, allopurinol, amiloroide HCl and chloramphenicol complexes with d-block metal ions have been discussed.[23—27)] For continuity, we have employed in this current article the coordination mode of (H_3Suz) complexes *via* some of d-block such as Mn(II), Hg(II), Cr(III), ZrO(II), VO(II) and Y(III). The solid products were isolated and characterized by elemental analysis CHN, molar conductance, magnetic moment and thermal analyses.

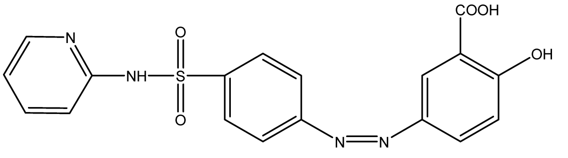

Fig. 1. Sulfasalazine (H_3Suz)

Experimental

Physical Measurements Carbon and hydrogen contents were determined using a Perkin-Elmer CHN 2400. The metal content was found gravimetrically by converting the complexes into their corresponding oxides.

Infrared spectra were recorded on Bruker FTIR Spectrophotometer (4000—400 cm^{-1}) in KBr pellets. The UV/VIS, spectra were studied in the DMSO solvent with concentration (1.0×10^{-3} M) for the H_3Suz and their complexes using Jenway 6405 Spectrophotometer with 1 cm quartz cell, in the range 800—200 nm. Molar conductances of the freshly prepared solutions of the H_3Suz complexes with 1.0×10^{-3} M in DMSO were measured using Jenway 4010 conductivity meter. Magnetic measurements were carried out on a Sherwood Scientific magnetic balance using Gouy method. ^{1}H-NMR spectra were recorded on a Varian Gemini 200 MHz spectrometer using DMSO-d_6 as solvent. Thermogravimetric analysis (TGA (thermo gravimetric analysis) and DTG (Differential thermo gravimetric analysis)) were carried out in dynamic nitrogen atmosphere (30 ml/min) with a heating rate of 10 °C/min using a Shimadzu TGA-50H thermal analyzer.

Antimicrobial Activity Test According to Gupta *et al.*,[28)] the hole well method was applied. The investigated isolates of bacteria were seeded in tubes with nutrient broth (NB). The seeded NB (1 ml) was homogenized in the tubes with 9 ml of melted (45 °C) nutrient agar (NA). The homogeneous suspensions were poured into Petri dishes. The holes (diameter 4 mm) were done in the cool medium. After cooling, 2 ml of the investigated compounds were applied using a micropipette. After incubation for 24 h in a thermostat at 25—27 °C, the inhibition (sterile) zone diameters (including disc) were measured and expressed mm. An inhibition zone diameter over 7 mm indicates that the tested compound is active against the bacteria under investigation.

The antibacterial activities of the investigated compounds were tested against *Escherichia coli* (Gram −ve), *Bacillus subtilis* (Gram +ve) and antifungal (tricoderma and penicillium activities).

Materials and Methods All chemicals used are analytical grade and purchased from Aldrich and Merck companies and H_3Suz drug was presented from Egyptian International Pharmaceutical Industrial Company (EIPI Co.). The complexes were prepared by mixing H_3Suz (2 mmol) and metal chlorides: $MnCl_2\cdot 4H_2O$, $HgCl_2$, $CrCl_3$, $ZrOCl_2\cdot xH_2O$, metal(II) sulfate: $VOSO_4\cdot xH_2O$ and metal(III) nitrate: $Y(NO_3)_3\cdot 6H_2O$ (1 mmol) in mixed solvent 50% (v/v) methanol–water (40 ml), then pH of the solution was adjusted to 8.0—9.0 with 0.1 M NaOH solution and the reaction mixture was stirred at 60 °C for 2 h and left to stand overnight. The precipitated complexes were filtered off, washed with MeOH and H_2O and dried *in vacuo* at room temperature under anhydrous $CaCl_2$.

---

* To whom correspondence should be addressed. e-mail: msrefat@yahoo.com

Results and Discussion

The elemental analysis (CHN) agrees quite well with the speculated structure of the colored H_3Suz complexes (Table 1). Manganese(II) complex is black color, mercury(II) complex is buff, the chromium(III) and vanadyl(II) complexes are dark brown, while the zirconyl(II) and yttrium(III) complexes are orange color. They are thermally stable above >250 °C, soluble in DMSO and DMF. The conductivity values measured in DMSO at room temperature located in the range of non-electrolytes[29] for Mn(II), Hg(II), ZrO(II), and VO(II)/HSuz complexes while the chromium(III) and yttrium(III) complexes behave as 1 : 1 electrolytes. The interpretation concerning the decreasing of conductivity values back to the deprotonation of both OH of carboxylic and OH of phenolic groups for the H_3Suz ligand. This assumption proves that free ligand acts as a bidentate fashion *via* carboxylic and phenolic groups and also attributed to the participation of carboxylic group as a monodentate chelate.

Magnetic moments were performed according to the Gauy method[30] and the value for the manganese(II) complex is 1.90 BM indicating that it has one unpaired electron. The chromium(III) complex has a magnetic moment equal 2.00 BM as predicted a low spin system with two unpaired of electrons hence, the Mn(II) and Cr(III) complexes formed have an octahedral configuration with d^2sp^3 hybrid orbital.

Infrared Spectra The infrared spectra of H_3Suz complexes are exhibited with the main of coordination bands which reveals to the mode of bonding are summarized in Table 2. Concerning the H_3Suz complexes, the main region in the infrared spectra of all complexes and the free H_3Suz ligand is (*ca.* 1700—1300 cm^{-1}) which was selected and assigned in Table 2 as follows:

In contrast to the assignments data of H_3Suz, Mn(II), Hg(II), Cr(III), ZrO(II), VO(II) and Y(III) complexes show no absorption band at 1677 cm^{-1}, characteristic of the ν(C=O) vibration of the carboxylic group (in case of free H_3Suz ligand), that is indicative of the involvement of the carboxylic group in the coordination with metal ion. The peaks at 1598 cm^{-1} (vs) for Mn(II)/HSuz, 1594 cm^{-1} (s) for Hg(II)/HSuz, 1598 cm^{-1} (vs) for Cr(III), 1595 cm^{-1} (vs) for ZrO(II)/HSuz, 1588 cm^{-1} (s) for VO(II)/HSuz and 1594 cm^{-1} (s) for Y(III)/HSuz complexes, respectively, are absent in the spectrum data of the free H_3Suz and can be assigned to the asymmetric stretching vibration of the carboxylate group, $\nu_{as}(COO^-)$. The spectra of $[Mn(HSuz)^{-2}(H_2O)_4]\cdot 2H_2O$, $[M(HSuz)^{-2}(H_2O)_2]\cdot xH_2O$ (M=Hg(II), ZrO(II) and VO(II), x=4, 8 and 6, respectively) and $[M(HSuz)^{-2}(Cl)(H_2O)_3]\cdot xH_2O$ (M=Cr(III) and Y(III), x=5 and 6, respectively) complexes also have medium to strong intensity band in the range of 1309—1327 cm^{-1}. This band is absent in spectrum of H_3Suz and interpretive to the symmetric vibration of the $\nu_s(COO^-)$ group.

Deacon and Phillips[31] have studied the criteria that can be used to distinguish between the three binding states of the carboxylate complexes. These criteria are: (i) $\Delta\nu > 200$ cm^{-1} (where $\Delta\nu = [\nu_{as}(COO^-) - \nu_s(COO^-)]$) this relation found in case of unidentate carboxylato complexes, (ii) bidentate or chelating carboxylato complexes, exhibit $\Delta\nu$ significantly smaller than ionic values ($\Delta\nu < 100$ cm^{-1}), and finally, (iii) bridging complexes show $\Delta\nu$ comparable to ionic

Table 1. Elemental Analyses and Physical Data of H_3Suz Complexes

Complexes	MW	mp/°C	Color	Magnetic moment	Content ((Calcd) Found)					Λ (S cm^2 mol^{-1})
					%C	%H	%N	%Cl	%M	
$[Mn(HSuz)(H_2O)_4]\cdot 2H_2O$	558.93	>300	Black	1.90	(38.64)	(4.29)	(10.01)	—	(9.82)	22
($C_{18}H_{24}N_4O_{11}S$ Mn)					38.14	4.30	9.97		9.75	
$[Hg(HSuz)(H_2O)_2]\cdot 4H_2O$	705	>300	Buff		(30.63)	(3.40)	(7.94)	—	(28.51)	24
($C_{18}H_{24}N_4O_{11}S$ Hg)					30.61	3.39	7.96		28.12	
$[Cr(HSuz)(Cl)(H_2O)_3]\cdot 5H_2O$	627.50	250	Dark brown	2.00	(34.42)	(4.46)	(8.92)	(5.65)	(8.28)	96
($C_{18}H_{28}N_4O_{13}S$ Cl Cr)					34.32	4.38	8.86	5.64	8.24	
$[ZrO(HSuz)(H_2O)_2]\cdot 8H_2O$	683.2	>300	Orange		(31.61)	(4.68)	(8.19)	—	(15.69)	23
($C_{18}H_{32}N_4O_{15}S$ ZrO)					31.40	4.70	8.22		15.52	
$[VO(HSuz)(H_2O)_2]\cdot 6H_2O$	606.94	>300	Dark brown		(35.58)	(4.61)	(9.22)	—	(11.02)	25
($C_{18}H_{28}N_4O_{13}S$ VO)					35.54	4.59	9.19		10.98	
$[Y(HSuz)(Cl)(H_2O)_3]\cdot 6H_2O$	682.40	>300	Orange		(31.65)	(4.39)	(8.20)	(5.20)	(13.02)	88
($C_{18}H_{30}N_4O_{14}S$ Cl Y)					31.18	4.58	8.68	5.48	13.16	

Table 2. Main IR Data of H_3Suz Complexes

Complexes	ν(O–H)	ν(C–O)	δ(OH)	ν_{as}(COO)	ν_s(COO)	$\Delta\nu$(COO)	ν(M–O)
Mn(II)	3385	1253	1357	1598	1309	289	516 454
Hg(II)	3422	1231	1350	1594	1327	267	512 486
Cr(III)	3422	1233	1358	1598	1313	285	524 434
ZrO(II)	3419	1241	1355	1595	1318	277	525 492
VO(II)	3357	1260	1357	1588	1310	278	452 422
Y(III)	3350	1263	1360	1594	1313	281	524 439

values ($\Delta\nu$ *ca.* 150 cm^{-1}). The observed $\Delta\nu$ for the all H_3Suz complexes is $>$200 cm^{-1} which confirms a unidentate interaction of the carboxylate group.

A broad diffuse band of strong to medium strong intensity in the 3500—3350 cm^{-1} region may be assigned to the OH stretching vibration for the coordinated and uncoordinated water molecules in the H_3Suz complexes. As is also difficult distinction between the ν(OH) of phenolic group of H_3Suz and the stretching vibrational bands of water molecules because of the overlapping values, and appear in one place.

To ascertain the involvement of OH of phenolic group of H_3Suz in the coordination process to be followed the stretching vibration bands of ν(C–O) in all H_3Suz complexes. Examination of the H_3Suz complexes found that the ν(C–O) is shifted to lower wavenumber from 1278 cm^{-1} in case of free ligand to 1230 to 1260 cm^{-1} in case of their complexes. This result indicates that the phenolic group is participated in the complexation and the H_3Suz ligand acts as bidentate. The lower shift of δ(OH) from 1393 cm^{-1} in the free H_3Suz ligand to 1360—1350 cm^{-1} in their complexes is the another factor confirmation wihch proves the involvement of OH phenolic group in the coordination process.

The presence of M–O stretching vibrations at two bands: 516 and 454 cm^{-1} for Mn(II)/HSuz, 512 and 486 cm^{-1} for Hg(II)/HSuz, 524 and 435 cm^{-1} for Cr(III)/HSuz, 525 and 492 cm^{-1} for ZrO(II)/HSuz, 452 and 422 cm^{-1} for VO(II)/HSuz and (524 and 439) for Y(III)/HSuz, respectively, supports coordination by H_3Suz ligand as a bidentate chelating agent *via* OH of carboxylic and phenolic groups.[32]

UV–VIS Spectra The UV/VIS spectra of H_3Suz and their complexes in DMSO are exhibited and the detected peaks are tabulated in Table 3. There are two absorption maxima peaks at ranged from 215—340 nm and 350—500 nm, assigned to π–π* and n–π* transitions within the organic moiety of H_3Suz ligand. The electronic absorption spectra of all H_3Suz complexes show a bathochromic shift rather than free ligand within n–π* transition region.[23—27] This shift attributed to the place of complexation and the change in the electronic configuration for the H_3Suz complexes formed. The electronic spectrum with respect to the Cr(III)/HSuz complex shows a weak absorption peak in the visible region probably due to spin-orbit forbidden transitions.

^{1}H-NMR Spectra The ^{1}H-NMR spectra presented the persuasive confirmation of the coordination modes. Thus, the ^{1}H-NMR spectra of both VO(II)/HSuz and Y(III)/HSuz complexes (Figs. 2A, B) on comparing with those of spectrum of the free H_3Suz[33] indicate that, H_3Suz ligand acts as bidentate ligand through the phenolic OH group and carboxylic OH group. ^{1}H-NMR spectra of vanadyl(II) and yttrium(III) complexes were carried out in DMSO-d_6 as a solvent, the data obtained are in agreement with the suggested coordination through the carboxylic and phenolic groups by absent the signals of two protons which exist in the free ligand at about δ=11.00 and 5.00 ppm, respectively, and due to different chemical environments the signals of aromatic protons at 6.00—8.00 ppm are present with decreasing in their intensities.

Thermal Analysis and Kinetic Studies It seemed of interest to evaluate the effect of heating on the thermal stability of the prepared complexes in the same trend as given previously.[23—27]

Table 3. Electronic Spectral Data of the Free H_3Suz Ligand and Its Complexes

Complexes	λ_{max} (nm)	ε (l mol^{-1} cm^{-1})	Assignment
H_3Suz	225	790	π–π* trans.
	280	3000	π–π* trans.
	290	1892	π–π* trans.
	360	2574	n–π* trans.
	390	1188	n–π* trans.
	415	1678	n–π* trans.
Mn(II)	225	3000	π–π* trans.
	290	2405	π–π* trans.
	360	2448	n–π* trans.
	385	2254	n–π* trans.
	440	2540	n–π* trans.
	480	2828	n–π* trans.
Hg(II)	215	3000	π–π* trans.
	240	946	π–π* trans.
	290	1786	π–π* trans.
	360	1330	n–π* trans.
	390	1123	n–π* trans.
	425	1771	n–π* trans.
Cr(III)	220	1389	π–π* trans.
	295	1749	π–π* trans.
	390	1153	n–π* trans.
	440	1576	n–π* trans.
ZrO(II)	220	3000	π–π* trans.
	295	3000	π–π* trans.
	340	1807	π–π* trans.
	390	1301	n–π* trans.
	460	2126	n–π* trans.
VO(II)	230	186	π–π* trans.
	270	324	π–π* trans.
	290	2086	π–π* trans.
	365	1220	n–π* trans.
	435	1893	n–π* trans.
Y(III)	220	167	π–π* trans.
	290	245	π–π* trans.
	360	1680	n–π* trans.
	390	1440	n–π* trans.
	430	2138	n–π* trans.

The results showed that the complexes lost its hydration water below 573 K. Within the temperature range 573—653 K the coordinated water molecules were liberated. The anhydrous complexes displayed the decomposition of the organic ligand within the temperature range 673—1073 K leading to metal oxide. The metal contents were calculated from the residual contents and were found to be in good agreement with the results of elemental analysis. The H_3Suz ligand melts at 552k with simultaneous decomposition. The thermal decomposition of (H_3Suz) occurs completely in two steps which were observed at 552 and 1025 K corresponding to loss of $C_4H_6N_4SO_3$ and $C_2H_8O_2$ (organic moiety) representing a weight loss of (obs=47.20%, calc=47.69) and (obs=16.50%, calc=16.00), respectively, then leaving residual carbon as final fragment.

[Mn(SuzH)(H_2O)$_4$]$\cdot$2H_2O complex was thermally decomposed in four successive decomposition steps within the temperature rang 313—1073 K. The first decomposition step (obs=6.69%, calc=6.44) within the temperature range 313—403 K, may be attributed to the liberation of the two hydrated water molecules. The second and third decomposition steps found within the temperature range 423—703 K

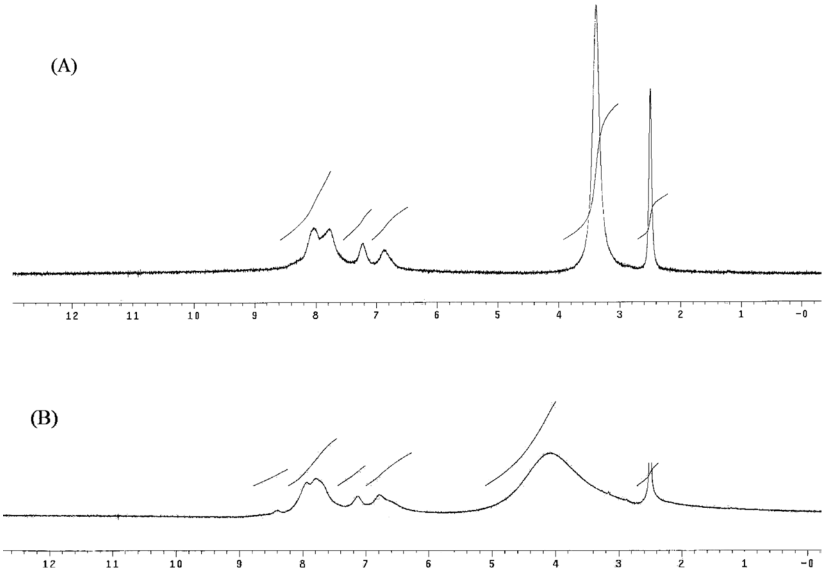

Fig. 2. ^{1}H-NMR Spectra of: (A) VO(II)/HSuz and (B) Y(III)/HSuz Complexes

(obs=12.43%, calc=12.88), (obs=13.82%, calc=13.77), which are reasonably accounted for by the removal of $4H_2O$ and $C_2H_7NO_2$ (organic moiety), respectively. The rest of H_3Suz molecule was removed on the fourth step within the temperature range 713—1073 K (obs=39.60%, calc=39.18). The decomposition of the ligand molecule ended with a final oxide residue of MnO and contaminated with residual carbon (27.23%, mass=154.93).

The TGA curve of $[Hg(SuzH)(H_2O)_2]\cdot 4H_2O$ complex indicates that the mass change begins at 367 K and continuous up to 1053 K. The first mass loss corresponds to the liberation of the four hydrated water molecules (obs=10.80%, calc=10.21). The second decomposition step occurs in the range 463—653 K and corresponds to the loss of $2H_2O+C_6H_8N_2SO_2$ (organic moiety) (obs=29.12%, calc=29.50). The final decomposition step occurs in the range 673—1073 K and corresponds to the loss of $C_4H_4N_2O_2$ (organic moiety) (obs=29.12%, calc=29.50). DTG profile shows three endothermic peaks. The first at 367 K corresponds to the melting of the complex, while the second at 527 K corresponds to the dehydration and decomposition of the complex. The third broad endothermic peak corresponds to the final decomposition of the organic ligand to the HgO+residual carbon atoms.

$[Cr(SuzH)(Cl)(H_2O)_3]\cdot 5H_2O$ was thermally decomposed in five successive decomposition steps within the temperature rang 323—1073 K. The first decomposition step (obs=7.39%, calc=7.17) within the temperature range 323—423 K, may be attributed to the liberation of two and half hydrated water molecules. The second and third decomposition steps found within the temperature range 443—813 K (obs=15.69%, calc=15.77), (obs=6.45%, calc=6.85), which are reasonably accounted for by the removal of $5.5H_2O$ and C_2H_5N (organic moiety), respectively. The rest of H_3Suz molecule was removed on the fourth and fifth steps within the temperature range 833—1073 K corresponds to the loss of C_2H_4N and $C_5H_3N_2SO_{3.5}Cl$ (organic moiety) (obs=6.56%, calc=6.69), (obs=33.86%, calc=34.18), respectively. The decomposition of the ligand molecule ended with a final oxide residue of $CrO_{1.5}$+contaminated carbon atoms.

$[ZrO(SuzH)(H_2O)_2]\cdot 8H_2O$ the complex is thermally stable up to 323 K and decomposition beyond this temperature as indicated by the first loss step in the TGA curve. The mass loss at 323 K corresponds to the loss of $2H_2O$ (obs=5.67%, calc=5.26). Continuous mass loss in the TGA curve beyond 333 K, 373 K, 433 K and 616 K, corresponds to the loss of $8H_2O$+NO. The rest of H_3Suz molecule was removed on the six and seven steps within the temperature range 723—1073 K corresponds to the loss of N_2+3H_2 and $0.5N_2+3H_2$ (obs=4.39%, calc=4.97), (obs=2.29%, calc=2.92), respectively. The DTG profile shows four endothermic peaks. The first and second peaks at 318, 373 K corresponds to the dehydration of the complex, while the third and fourth at 755, 1048 K corresponds to the final decomposition of the organic ligand to the $ZrOSO_4$+carbon atoms residue.

The complex $[VO(SuzH)(H_2O)_2]\cdot 6H_2O$ is thermally stable up to 306 K and undergoes decomposition beyond this temperature, as indicated by the first mass loss step in the TGA curve. The mass loss at 383 K corresponds to elimination of H_2O molecule (obs=2.50%, calc=2.96). Beyond 383 K continuous mass loss in the TGA curve has been observed up to 563 K which corresponds to elimination of the remained H_2O molecules and C_2H_2O (organic moiety) (obs=27.49%, calc=27.66). After this decomposition, the mass loss at 563—1073 K corresponds to removal of the rest of H_3Suz molecule. The DTG profile shows two endothermic and two broad exothermic peaks at 534, 560, 709 and 812 K. The first and the second endothermic peaks appear at 534 and 560 K corresponding to the dehydration of the complex, while the third and fourth exothermic peaks appear at 709 and 835 K corresponds to the decomposition of the organic ligand to the VO_2 (obs=13.78%, calc=13.66).

The complex $[Y(SuzH)(Cl)(H_2O)_3]\cdot 6H_2O$ is thermally stable up to 306 K and undergoes decomposition beyond this temperature, as indicated by the first mass loss step in the TGA curve. The mass loss at 368 K corresponds to elimination of $2.5H_2O$ molecules (obs=6.40%, calc=6.59). Beyond

Table 4. Thermal Data of H_3Suz and Its Complexes

Complexes	Steps	Temp. range (°C)	DTG peak (°C)	TGA weight loss (%)		Assignments
				Calcd	Found	
H_3SuZ	1	150—380	279	47.69	47.20	$C_4H_6N_4SO_3$
	2	400—800	752	16.00	16.50	$C_2H_8O_2$
						12C (residue)
$[Mn(HSuz)(H_2O)_4]\cdot 2H_2O$	1	40—130	54	6.44	6.69	$2H_2O$
($C_{18}H_{24}N_4O_{11}S$ Mn)	2	150—300	271	12.88	12.43	$4H_2O$
	3	340—430	400	13.77	13.82	$C_2H_7NO_2$
	4	440—800	560	39.18	39.60	$C_9H_5N_3SO_2$
						MnO+(7C resdiue)
$[Hg(HSuz)(H_2O)_2]\cdot 4H_2O$	1	50—180	94137	10.21	10.80	$4H_2O$
($C_{18}H_{24}N_4O_{11}S$ Hg)	2	190—380	254333	29.50	29.12	$2H_2O+C_6H_8N_2SO_2$
	3	400—800	780	15.88	16.12	$C_4H_4N_2O_2$
						HgO+(8C residue)
$[Cr(HSuz)(Cl)(H_2O)_3]\cdot 5H_2O$	1	50—150	60	7.17	7.39	$2.5H_2O$
($C_{18}H_{28}N_4O_{13}S$ Cl Cr)	2	170—380	325	15.77	15.69	$5.5H_2O$
	3	400—540	490	6.85	6.45	C_2H_5N
	4	560—640	580	6.69	6.56	C_2H_4N
	5	640—800	776	34.18	33.86	$C_5H_3N_2SO_{3.5}Cl$
						$CrO_{1.5}$+(9C residue)
$[ZrO(HSuz)(H_2O)_2]\cdot 8H_2O$	1	10—50	45	5.26	5.67	$2H_2O$
($C_{18}H_{32}N_4O_{15}S$ ZrO)	2	50—90	60	5.26	5.27	$2H_2O$
	3	90—140	100	2.63	2.19	H_2O
	4	140—270	160	5.26	5.73	$2H_2O$
	5	270—450	343	12.29	12.80	$3H_2O+NO$
	6	450—560	482	4.97	4.93	N_2+3H_2
	7	600—800	775	2.92	2.29	$0.5N_2+3H_2$
						$ZrOSO_4$+(18C residue)
$[VO(HSuz)(H_2O)_2]\cdot 6H_2O$	1	30—110	95	2.96	2.50	H_2O
($C_{18}H_{28}N_4O_{13}S$ VO)	2	110—250	240	4.44	4.29	$1.5H_2O$
	3	260—290	280	10.37	10.31	$3.5H_2O$
	4	290—350	332	12.85	12.89	$2H_2O+C_2H_2O$
	5	350—400	390	6.91	6.51	C_2H_2O
	6	400—450	440	9.22	9.32	C_2H_2NO
	7	450—550	530	14.49	14.94	C_2H_2NSO
	8	550—800	562	25.04	25.46	$C_{10}H_4N_2$
						VO_2 (residue)
$[Y(HSuz)(Cl)(H_2O)_3]\cdot 6H_2O$	1	30—95	85	6.59	6.40	$2.5H_2O$
($C_{18}H_{30}N_4O_{14}S$ Cl Y)	2	100—190	170	5.27	5.92	$2H_2O$
	3	200—280	260	6.59	6.31	$2.5H_2O$
	4	290—320	311	9.08	9.36	$2H_2O+C_2H_2$
	5	320—390	353	23.37	23.85	$C_5H_4N_2SCl$
	6	390—450	435	17.73	18.39	$C_6H_3NO_2$
	7	450—800	470	14.80	15.28	$C_5H_3NO_{1.5}$
						$YO_{1.5}$ (residue)

368 K continuous mass loss in the TGA curve has been observed up to 563 K which corresponds to removal of the remained H_2O molecules and C_2H_2 (organic moiety) (obs=21.59%, calc=20.94). After this decomposition, the mass loss at 593—1073 K corresponds to decomposition of the rest of H_3Suz molecule. The DTG profile shows two exothermic at 616 and 716 K. The first exothermic peak appears at 616 K corresponds to the elimination of $C_5H_4N_2SCl$ (organic moiety) (obs=23.85%, calc=23.37), while the second peak appears at 716 K corresponds to the decomposition of the organic ligand to the $YO_{1.5}$ (obs=16.57%, calc=16.54).

In the present investigation, the general thermal behaviors of the H_3Suz complexes in terms of stability ranges, peak temperatures and values of kinetic parameters, are shown in Table 4. The kinetic and thermodynamic parameters have been evaluated using the Coats–Redfern and Horowitz–Metzger equations.[34—36]

The entropy of activation, ΔS^*, was calculated. The enthalpy activation, ΔH^*, and Gibbs free energy, ΔG^*, were calculated from; $\Delta H^*=E^*-RT$ and $\Delta G^*=\Delta H^*-S^*$, respectively. The thermodynamic behavior of all complexes of H_3Suz with transition metal ions is non-spontaneously (more ordered) reactions (ΔS is negative value), endothermic reactions ($\Delta H>0$) and endergonic ($\Delta G>0$) during the reactions.

The thermodynamic data obtained with the two methods are in harmony with each other. The activation energy of Cr(III) and Hg(II) complexes is expected to increase in relation with decrease in their radii.[23,25—27] The smaller size of the ions permits a closer approach of the ligand. Hence, the E value in the second stage for the Cr(III) complex is higher than that for the other Hg(II) complex. The correlation coefficients of the Arrhenius plots of the thermal decomposition steps were found to lie in the range 0.9791 to 0.9999, showing a good fit with linear function. It is clear that the thermal decomposition process of all H_3Suz complexes is non-spon-

Table 5. Kinetic Parameters Using the Coats–Redfern (CR) and Horowitz–Metzger (HM) Operated for the H_3Suz and Its Complexes

Complexes	Stage	Method	Parameter					r
			E (J mol^{-1})	A (s^{-1})	ΔS (J mol^{-1} K^{-1})	ΔH (J mol^{-1})	ΔG (J mol^{-1})	
H_3Suz	1st	CR	1.31×10^5	2.13×10^{11}	-5.23×10	1.26×10^5	1.55×10^5	0.9791
		HM	1.47×10^5	9.89×10^{10}	-2.04×10	1.42×10^5	1.53×10^5	0.9993
Mn(II)	3rd	CR	7.85×10^4	1.45×10^5	-1.51×10^2	7.40×10^4	1.56×10^5	0.9902
		HM	8.44×10^4	1.12×10^6	-1.34×10^2	7.99×10^4	1.53×10^5	0.9961
Hg(II)	2nd	CR	1.25×10^5	2.57×10^{10}	-5.04×10	1.40×10^5	1.48×10^5	0.9997
		HM	1.34×10^5	2.76×10^{11}	-3.06×10	1.30×10^5	1.46×10^5	0.9985
Cr(III)	2nd	CR	9.37×10^5	3.57×10^5	-1.44×10^2	8.87×10^4	1.75×10^5	0.9960
		HM	6.09×10^5	2.98×10^6	-1.08×10^2	1.04×10^5	1.68×10^5	0.9999
ZrO(II)	3rd	CR	1.02×10^5	1.98×10^6	-1.30×10^2	9.71×10^4	1.78×10^5	0.9944
		HM	1.14×10^5	4.21×10^7	-1.05×10^2	1.09×10^5	1.74×10^5	0.9985
VO(II)	1st	CR	3.41×10^4	5.43×10^2	-1.94×10^2	3.11×10^4	1.02×10^5	0.9917
		HM	4.10×10^4	7.34×10^3	-1.73×10^2	3.80×10^4	1.01×10^5	0.9990
Y(III)	1st	CR	5.45×10^4	8.67×10^5	-1.33×10^2	5.15×10^4	9.91×10^4	0.9996
		HM	6.14×10^4	1.29×10^7	-1.10×10^2	5.84×10^4	9.79×10^4	0.9998

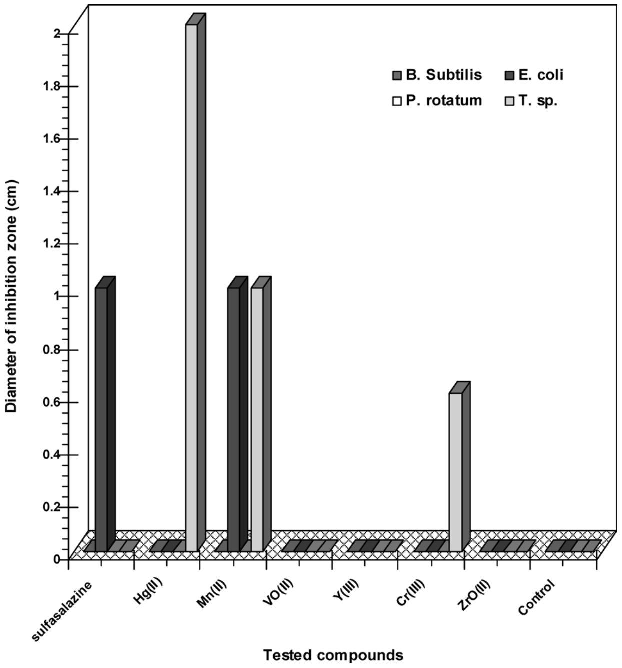

Fig. 3. Microbial Test for H_3Suz and Its Complexes

taneous, *i.e.*, the complexes are thermally stable.

The thermograms and the calculated thermal parameters for the complexes show that the stability of these complexes depends on the nature of the central metal ion. It can be seen from the curves that the thermal stability of ZrO(II) complex is higher than that for the corresponding VO(II) complex with the same ligand. The decomposition temperature of ZrO(II) complex lies at 1048 K, but the VO(II) complex decompose to the oxide at 835 K. The thermal stability of the metal complexes was found to increase periodically with increase in atomic number of the metal and the larger value of charge/radius ratio.[37)]

Antimicrobial Activity Anti bacterial and antifungal activities of the ligand and its complexes were carried out against the *Escherichia coli* (Gram −ve), *Bacillus subtilis* (Gram +ve) and antifungal (tricoderma and penicillium activities). The results of the antimicrobial test are shown in Fig. 3. The antimicrobial activity was estimated on the basis of size of inhibition zone around dishes. The ligand and complexes were less active against *Bacillus subtilis* and penicillium, whereas Hg(II)/HSuz is more active rather than Cr(III) and Mn(II) complexes against tricoderma.

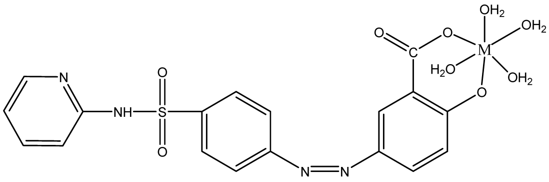

Fig. 4A. Structure of Mn(II)/HSuz Complex

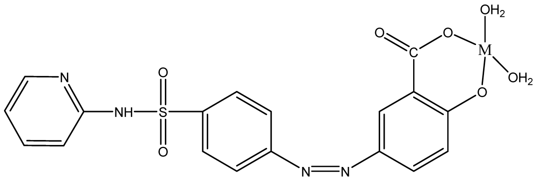

Fig. 4B. Structure of M(II)/HSuz Complex (Where M=Hg(II), ZrO(II) and VO(II))

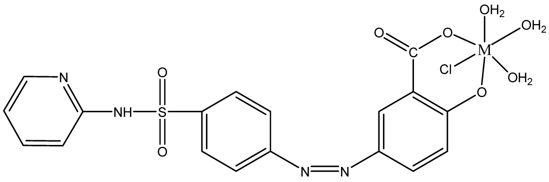

Fig. 4C. Structure of M(III)/HSuz Complex (Where M=Cr(III) and Y(III))

For example, the antifungal activity of Hg(II)/HSuz complex was evaluated against *Tricoderma* sp. according to the adopted method of Gupta *et al.*,[28)] with some modifications. It could be concluded that, the minimum inhibitory concentration (MIC) of the Hg(II) complex against the tested fungal isolated is 40 μg/ml with further increasing in the concentration of the tested complex a detectable suppression in fungal growth was observed.

Structure of the Sulfasalazine Complexes Finally, it is concluded that from elemental analysis, magnetic properties and IR and ^{1}H-NMR spectra, the H_3Suz behaves as a bidentate ligand coordinated to the metal ions Mn(II), Hg(II), Cr(III), ZrO(II), VO(II) and Y(III) through the phenolic OH group and carboxylic OH group (Fig. 4).

References

1) Sutherland L., Roth D., Beck P., Cochrane Database Syst. Rev. 2000; CD000543.
2) Hanauer S. B., Sandborn W. J., Kornbluth A., *Am. J. Gastroenterol.*, **100**, 2478—2485 (2005).
3) Bell C. M., Habal F. M., *Am. J. Gastroenterol.*, **92**, 2201—2202 (1997).
4) Diav-Citrin O., Park Y. H., Eerasuntharam G. V., *Gastroenterology*, **114**, 23—28 (1998).
5) Zaki A., Schreiber E. C., Weliky I., Knill J. R., Hubsher H. J., *J. Clin. Pharmacol.*, **14**, 118—126 (1974).
6) Klostersky J., Danean D., Weerts D., *Chemotherapy*, **18**, 191—196 (1973).
7) Anacona J. R., *J. Coord. Chem.*, **54**, 355—365 (2001).
8) Lozano J., Borras J., *J. Inorg. Biochem.*, **31**, 187—195 (1987).
9) Abdel-Gawad F. M., El-Guindi N. M., Ibrahim M. N., *J. Drug Res.*, **17**, 197—202 (1987).
10) Helaleh M. I. H., Nameh E. S. M., *An. Quim. Int. Ed.*, **94**, 160—165 (1998).
11) Sorenson J. R. J., *J. Med. Chem.*, **19**, 135—148 (1976).
12) Brown D. H., Lewis A. E., Smith W. E., Teape J. W., *J. Med. Chem.*, **23**, 729—734 (1980).
13) Williams D. R., "The Metals of Life," Van Nostrand Reinhold, London, 1971.
14) Ruiz M., Perello L., Ortiz R., Castineiras A., Maichlemossmer C., Canton E., *J. Inorg. Biochem.*, **59**, 801—810 (1995).
15) Chen Z.-F., Kang S., Shi S.-M., Abrahams B. F., Liang H., *J. Mol. Struct.*, **882**, 134—139 (2008).
16) Chen Z.-F., Kang S., Liang H., Yi F., Yu K.-B., Xiong R.-G., You X.-Z., *Appl. Organometal. Chem.*, **17**, 887—888 (2003).
17) Wang X.-S., Song Y.-M., Xiong R.-G., *Chin. J. Inorg. Chem.*, **21**, 1277—1283 (2005).
18) Yuan R.-X., Shi J.-D., Yang G.-W., *Chin. J. Inorg. Chem.*, **22**, 877—882 (2006).
19) Kang S., Chen Z.-F., *J. Guangxi Normal University*, **26**, 789—793 (2006).
20) Mukherjee G. N., Basu S., Ghosh T., *J. Indian Chem. Soc.*, **70**, 1043—1050 (1993).
21) Golzar Hossain G. M., Amoroso A. J., Banu A., Malik K. M. A., *Polyhedron*, **26**, 967—974 (2007).
22) Tabassum S., Arimand F., Rafiqi S. H., *Main Group Metal Chem.*, **19**, 245—252 (1996).
23) Abd El-Wahed M. G., Refat M. S., El-Megharbel S. M., *Spectrochim. Acta A*, **70**, 916—922 (2008).
24) Refat M. S., *J. Mol. Struct.*, **842**, 24—37 (2007).
25) Abd El-Wahed M. G., Refat M. S., El-Megharbel S. M., *J. Mol. Struct.*, *in press* (2008).
26) Abd El-Wahed M. G., Refat M. S., El-Megharbel S. M., *J. Mol. Struct.*, *in press* (2008).
27) Abd El-Wahed M. G., Refat M. S., El-Megharbel S. M., *Mens Agitat.*, **3**, 33—41 (2008).
28) Gupta R., Saxena R. K., Chatarvedi P., Virdi J. S., *J. Appl. Bacteriol.*, **78**, 378—381 (1995).
29) Geary W. J., *Coord. Chem. Rev.*, **7**, 81—122 (1971).
30) Lever A. B. P., "Inorganic Electronic Spectroscopy," 4th ed., Elsevier, London, 1980, p. 481.
31) Deacon G. B., Phillips R. J., *Coord. Chem. Rev.*, **33**, 227—250 (1980).
32) Nakamoto K., "Infrared and Raman spectra of Inorganic and Coordination Compounds," 4th ed., Wiely, New York, 1986.
33) Doraswamy G., *J. Indian Chem. Soc.*, **23**, 278—282 (1946).
34) Coats A. W., Redfern J. P., *Nature* (London), **201**, 68—69 (1964).
35) Horowitz H. W., Metzger G., *Anal. Chem.*, **35**, 1464—1468 (1963).
36) Osowole A. A., Woods J. A. O., Fagade O. E., Odunola O. A., *Biosci. Res. Commun.*, **14**, 531—535 (2002).
37) Malik W., Tuli G. D., Madan R. D., "Selected Topics in Inorganic Chemistry," Chand and Co., Ltd., New Delhi, 1984.